Chapter 4
Results and Discussion

4.1 Hydrodynamics and Mass Transfer behavior

This section explains the hydrodynamics and mass transfer behavior in the submerged and airlift filters. The hydrodynamics and mass transfer in the trickling filter was significantly different from other filters and there this will not be included in this study.

4.1.1 Gas holdups in the various filters

Gas holdups in Riser and Downcomer

Experiment indicated that gas holdups in downcomer of the airlift filters (both packed bed and fluidized bed) were quite low and could not be detected by the technique employed in this work. Hence, gas bubbles in the system only resided in the riser and gas-separator of the system. Moreover, the gas-separator (the top part above the draft tube where gas disengaged from the system) only possessed small fraction of the overall volume of the system and it was assumed that the gas holdup in this section was the same as that in riser. Hence, the overall gas holdup in the system could be computed from all the bubbles in the riser. However, the gas holdup in this work was measured only in the downcomer by the hydrostatic pressure difference method (manometer) and the volume displacement method. The later method gave the information on overall gas holdup. Therefore, if one needs to know the riser gas holdup, the mass balance on the gas phase could be performed on the system and the results are displayed in Figure 4.1. The effect of various factors on the gas holdup will subsequently explained in later sections.

Overall gas holdups

Figure 4.2 illustrates that the overall gas holdups in all types of contactors increased with an increase in the gas superficial velocity. This is not uncommon as higher gas throughputs led to higher bubble concentration in the filter which in turn resulted in a higher gas holdups.

However, the extent at which the gas holdup increased with superficial gas velocity in each type of filter was different from each other. This section provides possible reasons of why this happens.

In the submerged filter, since there was no partitioning of the filter, the gas was supplied through the whole cross sectional area of the 10 cm diameter column. The actual gas velocity in this system was therefore lower than the other systems where the column was partitioned into the riser and downcomer. In both airlift filters, the gas was only supplied through the cross sectional area of riser (6 and 8 cm depending on the size of the draft tube). The experiment indicated that downcomer gas holpups in all cases were close to zero (as explained earlier). The smaller cross sectional area means that the actual gas velocity (in riser) was higher than the actual velocity in the submerged filter. A faster gas velocity led to a smaller bubble residence time in the system, i.e. gas bubbles left the system more rapidly. Therefore the gas holdups in these airlift systems were lower than that observed in the submerged filter.

For the airlift systems, it was found that, at the same condition, the overall gas holdup in the fluidized bed airlift filter was lower than that in the packed bed airlift filter (Fig. 4.1). To explain this finding, it is recommended that the configuration of each system was described in more detail. The packing used in fluidized bed airlift was made by grinding the plastic bioball using the plastic grinder [Petroleum and Petrochemical College, Chulalongkorn University]. The packing obtained from this grinder was cubic in shape with the mean diameter of approximately 3 mm. This packing, when in the airlift filter, was still quite heavy and it required a rather high gas throughput to create the fluidized bed condition. A common practice for nitrification is to supply air at high flowrate. However, Silapakul, 2002 demonstrated that the system should only be operated at low gas throughput (< 2.5 cm/s). This was to make sure that the medium from the nitrification process did not have high level of dissolved oxygen which could be detrimental to the downstream denitrification process. Hence, the nitrification in this work would only be operated with superficial velocity in a low range of 1.0-2.3 cm/s. The top range was found to be just adequate for the packing employed in this work to fluidize (for the airlift filter with A_d/A_r of 2.78). At a relatively low superficial velocity, the fluidized bed was not complete and there still existed the overlapping of packings which is hereafter called "still bed condition" in this thesis. During this stage, bubble was blocked underneath the packing layer of the airlift filter. High pressure drop in this condition caused bubble to pass through the bed in a large size which reduced the residence time of the bubble in the contactor. Hence, low gas holdup was observed. causing bubble being unable to get through the filter. Since the bubble concentration is low, overall gas holdup in fluidized bed is lower than that in packed bed airlift filter.

For the airlift system, the ratio between the cross sectional areas of downcomer and riser (A_d/A_r) could be significant in determining the overall gas holdup in the system. Experiment illustrated that the system with A_d/A_r of 2.78 had a lower gas holdup than the system with A_d/A_r of 1.57. This experiment was only performed at a superficial velocity of 2.3 cm/s as this velocity provides the highest nitrification rate (see later sections).

Normally, the airlift system with large A_d/A_r (small riser area) produced high liquid velocity and this leads to a smaller gas holdup. This was in good agreement with the experimental finding described in the previous paragraph. However, the two experimental setups did not have the same number of plastic bioballs. The 1.57 A_d/A_r contained 200 bioballs whilst the 2.78 only had 100 bioballs. This was because it was not possible to put two hundred bioballs into the riser of the 2.78 A_d/A_r airlift system (too small riser). Hence, the effect of A_d/A_r on the hydrodynamics of the airlift systems could not be properly quantitatively concluded from this experiment.

It should be noted here that the actual nitrification experiments, however, might have to be performed at different condition for the various filters. The airlift system with A_d/A_r of 2.78 had to be operated with higher gas throughput (u_{sg} = 2.3 cm/s) to ensure a fluidized condition.

4.1.2 Liquid velocities in the various filters

Riser liquid velocity in the packed bed airlift filter could be determined using the technique described in Section 3.3.2 and the results were shown in Figure 4.3. In the fluidized bed airlift filter, on the other hand, the liquid velocity could not be easily determined using the same technique. Therefore a semi-theoretical method proposed by Livingston and Zhang [1993] was applied here and the detail follows:

From Energy conservation rule:

Rate of energy input into reactor = rate of energy dissipation

or in mathematical expression:

$$E_i = E_R + E_D + E_B + E_T + E_F \tag{4-1}$$

where E_i = energy input due to isothermal gas expansion

$= QP_h \ln\left(1 + \frac{\rho_D g h_D}{P_h}\right)$

E_R = energy dissipation due to wakes behind bubbles in the riser

E_D = energy loss due to stagnant gas in the downcomer

E_B = energy loss due to fluid turn around at the bottom of filter

E_T = energy loss due to fluid turn around at the top of filter

E_F = energy loss due to friction in the riser and the downcomer

Newitt *et al.* [1961] measured frictional losses in a vertical pipe in which various solid particle mixtures were being conveyed in water. They showed that at solid volume fractions of less than 15% (which corresponded to the operational parameters typically employed in TPAL reactors - 0.7 for A_d/A_r 1.57 and 0.5 for A_d/A_r 2.78) the increase in head loss over that for normal liquid flow is less than 30%; thus, wall friction is assumed to be negligible in TPAL systems as well. It is further assumed that the head loss at the flow reversals can be written in terms of the densities of the pseudo-homogeneous continuous phases as

$$P_{loss} = \frac{1}{2}\rho_{HD} K_B V_{LD}^2 + \frac{1}{2}\rho_{HR} K_T V_{LR}^2 \tag{4-2}$$

where K_B = head loss coefficients for fluid reversals at the bottom of filter

K_T = head loss coefficients for fluid reversals at the top of filter

V_{LR} = actual velocity of liquid in riser (m/s)

V_{LD} = actual velocity of liquid in downcomer (m/s)

From continuity principals, we can write V_{LR} and V_{LD} in terms of ε_{GD}, ε_{GR}, ε_{SR}, ε_{SD} and U_{LR} :

$$V_{LR} = \frac{U_{LR}}{1-\varepsilon_{GD}-\varepsilon_{SD}} \tag{4-3}$$

$$V_{LD} = \frac{U_{LD}}{1-\varepsilon_{GD}-\varepsilon_{SD}} \tag{4-4}$$

In our system, a metal sieve was installed at the top of the riser and it was not possible for the packing to leave the riser. As a result, no solid fraction was present in the downcomer or ε_{SD} was equal to zero. Hence,

$$V_{LD} = \frac{U_{LD}}{1-\varepsilon_{GD}} \tag{4-5}$$

Furthermore, the equation of continuity for the liquid flow between the riser and downcomer leads to:

$$A_R(1-\varepsilon_R-\varepsilon_S)V_{LR} = A_d(1-\varepsilon_D)V_{LD}$$

or
$$V_{LD} = \frac{A_R}{A_D}\frac{(1-\varepsilon_R-\varepsilon_S)}{(1-\varepsilon_D)}V_{LR} \tag{4-6}$$

Replacing V_{LR} from Eq. 4-3 yields the following expression.

$$V_{LD} = \frac{A_R}{A_D}\frac{(1-\varepsilon_R-\varepsilon_S)}{(1-\varepsilon_D)}\frac{U_{LR}}{(1-\varepsilon_R-\varepsilon_S)}$$

or
$$V_{LD} = \frac{U_{LR}}{(1-\varepsilon_D)}\frac{A_R}{A_D} \tag{4-7}$$

From Eq. 4-2, the energy losses in the top and bottom sections of the airlift filter could be calculated in exactly the same way as for pipe flow. Thus

$$E_B + E_T = \frac{1}{2}\left[\rho_{HD}K_B V_{LD}^2 A_D(1-\varepsilon_D) + \rho_{HR}K_T V_{LR}^2 A_R(1-\varepsilon_R-\varepsilon_S)\right] \tag{4-8}$$

Substitute Eqs. 4-3 and 4-7 into 4-8 gives:

$$E_B + E_T = \frac{1}{2}U_{LR}{}^3 A_R\left[\frac{K_T\rho_{HR}}{(1-\varepsilon_R-\varepsilon_S)^2} + \left(\frac{A_R}{A_D}\right)^2\frac{K_B\rho_{HD}}{(1-\varepsilon_D)^2}\right] \tag{4-9}$$

Energy dissipation due to the wakes behind the bubbles in the riser can be obtained from: [Chisti *et al.*, 1988]

$$E_i = E_R - \underbrace{\rho_L g H_D (1-\varepsilon_R) U_{LR} A_R}_{\text{pressure energy loss}} + \underbrace{\rho_L g H_D U_{LR} A_R}_{\text{potential energy gain}} \tag{4-10}$$

Hence

$$E_R = E_i - \rho_L g H_D U_{LR} A_R \varepsilon_R \tag{4-11}$$

Energy loss arising from the drag of gas on liquid in the downcomer (E_D) is obtained by performing an energy balance on the downcomer, using the downcomer liquid as the control volume:

$$0 = E_D + \underbrace{\rho_L g H_D (1-\varepsilon_D) U_{LD} A_D}_{\text{pressure energy gain}} - \underbrace{\rho_L g H_D U_{LD} A_D}_{\text{potential energy loss}} \tag{4-12}$$

or

$$E_D = \rho_L g H_D U_{LD} A_D \varepsilon_D \tag{4-13}$$

Substitute Eqs. 4-9, 4-11 and 4-13 into Eq. 4-1 and rearrange for U_{LR}:

$$U_{LR} = \left(\frac{2gH_D\left[\rho_{HD} - \rho_{HR}(1-\varepsilon_{GR})\right]}{\dfrac{\rho_{HR}K_T}{(1-\varepsilon_{GR}-\varepsilon_{SR})^2} + \rho_{HD}K_B\left(\dfrac{A_R}{A_D}\right)^2 \dfrac{1}{(1-\varepsilon_{GD})^2}} \right)^{0.5} \tag{4-14}$$

Experimental results shown in Figure 4.4 demonstrated that riser liquid velocity increased as the superficial gas velocity increased. Likewise, this trend can be observed for the calculated riser velocity.

The calculation shows that the liquid velocity in the fluidized bed airlift filter should be higher than that in the packed bed airlift filter. This was because the condition in fluidized bed filter was theoretically more appropriate for the liquid flow than the packed bed. Experiment results, however, did not correspond well with the calculation. At low gas superficial velocity (in the fluidized bed airlift filter at A_d/A_r of 1.57), the liquid velocity was found to be relatively low (at the same level as the packed bed). At this point, it is reminded that the fluidized bed filter employed in this work still was not operated at the full fluidized condition (as described earlier). The "still bed condition" was considered to be the reason for this contrasting incidence. At this condition, the density of the packing was high as a large fraction of particles were still not fluidized and hence acted like a resistant layer for the flow of gas. As a result, bubbles accumulated at the bottom of the column (underneath the packing) and formed large bubbles. These large bubbles when large enough would lift the dense packing up the column before broke up and dispersed through the riser and left the column in a very short time period. As these large bubbles left the system the particles fell to the bottom and formed a still bed again. When the gas superficial velocity was adequately high (e.g. in airlift fluidized bed with A_d/A_r of 1.57 and at u_{sg} of more than 1.5 cm/s), the system could produce a perfect fluidized bed condition where no still packing was found at the bottom of the column. And this condition would result in a higher liquid velocity than that found in packed bed airlift filter (see Fig. 4.4). One should notice that liquid velocity obtained from the experiment was not equal to the calculation. The liquid velocity measurement in the fluidized bed was achieved by measuring the time the color tracer required the move between any two points in the riser. The high turbulence condition in the riser, however, caused the color tracer to disperse quickly and it was difficult to visually detect the color in the column. Therefore it was highly possible that the measurement was not of high accuracy. Although the error bar indicated low humanly error, systematic error might be the true cause of this discrepancy. This error was more obvious in the system with A_d/A_r of 2.78 (Fig. 4.5). In this experiment, the small riser caused extremely high turbulence in the system and it was not possible at all to detect the color in the riser. Hence, the experiment was performed by measuring the velocity in the downcomer instead. However, the large area in downcomer caused the color to disperse through the downcomer cross sectional area, resulting in a low observed liquid velocity. It was concluded here that new experimental method for the liquid velocity measurement needed to be developed for this specific purpose.

It is worth noted here that the experimentally systematic error in liquid velocity measurement could be encountered in the airlift system with large downcomer, i.e. in the system with A_d/A_r of 2.78. This error was due to the dispersion of the color tracer into the large space of downcomer. In this work, the calculated values were further employed in other purposes.

4.1.3 Overall volumetric mass transfer coefficient in the various filters

The overall volumetric mass transfer coefficient, k_La, consists of two quantities: k_L or mass transfer coefficient, and the specific surface area where the mass exchange takes place, a. The value of k_L depends on the turbulence level in the liquid and also is a function of the difference between gas and liquid velocity, or what is called "slip velocity". The a value depends on the size of the bubble where smaller bubbles give large value of a. According to Figure 4.6, the overall volumetric mass transfer coefficient was found to vary directly with the superficial gas velocity. An increase in the gas velocity led to a higher gas holdup and this increased the turbulence in the system and the k_La increased. The interesting point is therefore lies at the comparison between the performance of submerged filter and the two airlift filter systems.

In the submerged filter, there was no partition for the back-flow of liquid and hence the behavior of the filter was similar to that of bubble columns where the net liquid velocity was zero. Therefore the difference between the liquid and gas velocities was considered to be the greatest among the three filters. This led to a higher k_L in the submerged filter. Although the a value in the submerged and the packed bed airlift filters could not be both quantitatively and qualitatively compared, this increase in k_L was believed to be the reason of high k_La in the submerged filter.

Poor performance again was found for the fluidized bed airlift system. In fluidized bed, the "still bed condition" prevented the good distribution of the bubbles and also caused a formation of large bubbles at the bottom of the column. In addition, from time to time, large bubbles passed through the dense still packing before quickly left the system. This situation was bad for the gas-liquid mass transfer as there was not enough surface area for the transfer (very small a). In the fluidized bed airlift filter at A_d/A_r of 2.78, the system was found to operated in a more proper fluidizing condition, i.e. the particles were more homogeneously distributed in the riser. At this condition, the k_La was found to be much higher and in the level comparable to the packed bed airlift filter (see Fig. 4.6).

4.2 Nitrification performance

4.2.1 Comparative performance between the four filters

This section compares the performance of the tricking filter, the submerged filter, the packed bed airlift and fluidized bed airlift filters in the removal of ammonia from the synthetic wastewater. The wastewater was prepared at a reasonably high concentration of ammonia to represent the actual case where there was a high accumulation of ammonia from the marine operation. The experiment on the trickling filter was only conducted as a base case as this type of filter is by far the most common filter used in the nitrogen removal facilities. However, the operation of the trickling filter was totally different from the operation of other systems and would only make use of the nitrification rate without looking into the detail of the operation of this system.

A number of experiments were carried out at different level of gas throughputs. Each experiment, however, was performed in a semi-continuous mode, in which the system was run continuously for a reasonably long period but ammonia was only added to the system at a certain time, usually when the ammonia was totally removed from the system, the new batch of ammonia was then added. The concentrations of ammonia, nitrite and nitrate were monitored during the experiment and examples of the results are given in Figure 4.7 In the report, however, it was proposed that every time ammonia was added into the system, the system would be considered as a new batch (although there was absolutely no other changes in the system). In other words, when ammonia was completely removed from the first run, new ammonia was added into the system and this was called a new batch.

Figure 4.8 illustrates the comparative performance of the four systems employed in this work. It is obvious that the trickling filter was the poorest in terms of specific ammonia removal rate. In fact, the trickling filter, at times, was able to treat ammonia at the same rate as other systems. However, this specific system requires large space and also a large number of bioballs so that the wastewater could be treated at the same rate as the others. All other systems, i.e. submerged filter, packed bed airlift filter, and fluidized bed airlift filter performed better than the trickling filter as long as the specific ammonia removal rate was concerned.

Before proceeding with further discussion, it is worth noting again here that one factor that played the main role of removing most nitrogen was the type and quantity of microorganisms in the system. These microorganisms were responsible for the oxidation of ammonia into nitrite and eventually into nitrate (as described in Chapter 2). The nitrification is the aerobic reaction where oxygen is the significant factor for the complete degradation of ammonia nitrogen. The system with a high gas-liquid mass transfer is therefore more appropriate for the nitrification reaction as oxygen from the gas phase can be more easily transferred into the liquid phase. The quantity of microorganism is also one of the important factors. Systems with large quantity of microorganism could work at a higher nitrification rate than system with small quantity of microorganism. Nitrifying bacteria, however, like to attach themselves to the surface in the reactor. That is the reason for supplying plastic bioballs into the system. The quantity of the nitrifying bacteria, hence, depends on the thickness of the biofilm formed on the surface of these bioballs. Unfortunately, for all the time period of this experiment, the thickness of the biofilm could not be measured due to experimental limitation.

Figure 4.8 is the results from the various systems where the A_d/A_r of the airlift filters was fixed at 1.57. As stated earlier, higher batch numbers means that the system was left running for a long time period. This specific experiment could be grouped into 3 phases: (a) batch number 1-5: operated with a superficial velocity of 1.7 cm/s; (b) batch number 6-10: operated with a superficial velocity of 2.3 cm/s; and (c) batch number 11-15: operated with a superficial velocity of 1 cm/s. The tricking filter system, on the other hand, was only operated specifically at a liquid circulation flow rate of 0.103 m/s but with the same operation time with batch number 1-5. The fluidized bed airlift filter system, the packed bed airlift filter system, and the submerged filter was operated at all phases.

The time profile of the ammonia removal rate for the three filters (submerged, packed bed airlift, and fluidized bed airlift filters) in Figure 4.7 indicated the performance of these systems was better with time. In other words, at the start of the experiment, none of the filters possessed high removal rate, but at later batches, the removal rate was observed to be much higher than the initial rate. This was because, at the start, there was only small number of microorganisms were presented in the system and the removal rate at which these microorganisms worked was limited by the number of cell that could do the degradation. As time passed, the microorganisms grew in number (thicker biofilm was expected) and a faster removal rate could be observed. However, the specific removal rate seemed to reach the maximum achievable at the later run (Batch # 4-5, which the same condition). This limitation was believed to be due to the oxygen available for the nitrification. To prove this hypothesis, the three systems were operated with higher gas throughput (increase from 1.7 cm/s in Batch # 1-5 to 2.3 cm/s in Batch # 6-10) to ensure that more oxygen could be transferred into the medium (as higher gas-liquid mass transfer could be obtained at this condition). The results were as anticipated, i.e. the nitrification rate started to increase. This rate increased up to a certain point where it was leveled off again. It was expected again that this was because the limitation on the oxygen mass transfer. This time, the aeration was turned down (to 1 cm/s in Batch # 11-15) and the nitrification rate subsequently declined. Two important messages are obtained from this specific experiments: (i) the system needed some time for start-up as the microorganisms had to increase their quantity to be able to cope with the ammonia load, and (ii) the system could easily be limited by the availability of oxygen. Nevertheless, the nitrification rates obtained from these experiments were much higher than the rate commonly required in the actual application (treatment of shrimp pond effluent – see Silapakul, 2002). These rates were therefore considered adequate for this specific purpose.

The time profiles of nitrite in fluidized bed and nitrate in fourth and fifth filter (fluidized bed, packed bed and submerged filter) airlift filter at the superficial velocity of 1.7 cm/s were presented in Figures 4.10 - 4.15 (including the time profile of ammonia). Initially, the ammonia should be converted into nitrite. Nitrite would then be converted to nitrate. This was illustrated in the mentioned figures as when ammonia was degraded, the nitrite concentration increased. The nitrite concentration then dropped as it was converted to nitrate and the nitrate profile went up with time. Nitrate was accumulated in the system as it was not converted to other nitrogen compound species. At higher gas throughput (like in Batch # 6-10), the concentration of nitrate was higher than the concentration at low gas throughput (Batch # 1-4). This was due to the different quantity of ammonia that underwent the nitrification reaction in the two conditions. In actual treatment system, this nitrate will be further converted into nitrogen gas in the anoxic denitrification step. This is not the objective of this work and will not be included here.

4.2.2 Effect of A_d/A_r to total ammonia nitrogen removal rate in the two airlift filters

The effect of A_d/A_r on the total ammonia nitrogen removal rate for the two airlift systems could be summarized along with each other as they presented the same trend (see Figs. 4.8 and 4.9). Experiments showed that the nitrification rate for the two airlift filters decreased with increasing A_d/A_r. This was not surprising as the hydrodynamic experiment showed that the gas-liquid mass transfer in the airlift filters decreased with the A_d/A_r. This means that less oxygen could be transferred from gas to liquid phases and, as a result, the nitrification rate decreased. However, the overall performances of the two airlift systems were different at the two A_d/A_r. This is described as follows.

It could be observed from this work that the fluidized bed performed better at high A_d/A_r. The ammonia removal rate from the fluidized bed airlift system with A_d/A_r of 2.78 was higher than that from the packed bed, whilst the opposite was found at A_d/A_r of 1.57 (Fig. 4.8). This was because the fluidized bed condition could be achieved better in the airlift filter with small riser (large A_d/A_r). In this system, only a low gas superficial velocity was needed to create the fluidized bed condition while in the system with large riser needed higher gas velocity to obtain the same fluidizing condition. However, the condition employed in this work led to a "still bed condition" in the fluidized bed system with large riser (as described earlier). Therefore the removal rate in the fluidized bed at A_d/A_r of 1.57 was not comparable to the packed bed airlift filter.

It is noted also that the draft tube of the airlift filter could only be built in two sizes. This was because the outer column was only 10 cm and there was not variety of acrylic tube diameter available commercially in smaller than 10 cm (already used the ones with 6 and 8 cm as draft tubes). The experiment was therefore limited to only two A_d/A_r.

4.2.3 Effect of superficial gas velocity to total ammonia nitrogen removal rate

In the discussion on the hydrodynamics and mass transfer, it was concluded that the gas holdup and overall volumetric mass transfer coefficient increased with the superficial gas velocity in all systems. This means that more oxygen from gas phase was able to transfer to the liquid phase. Therefore, it was anticipated that the ammonia removal rate would increase with the increase in the superficial gas velocity, and the experiments already proved this statement as discussed earlier in this chapter. However, the extent at which the removal rate increased depended on several factors as also stated in this chapter.

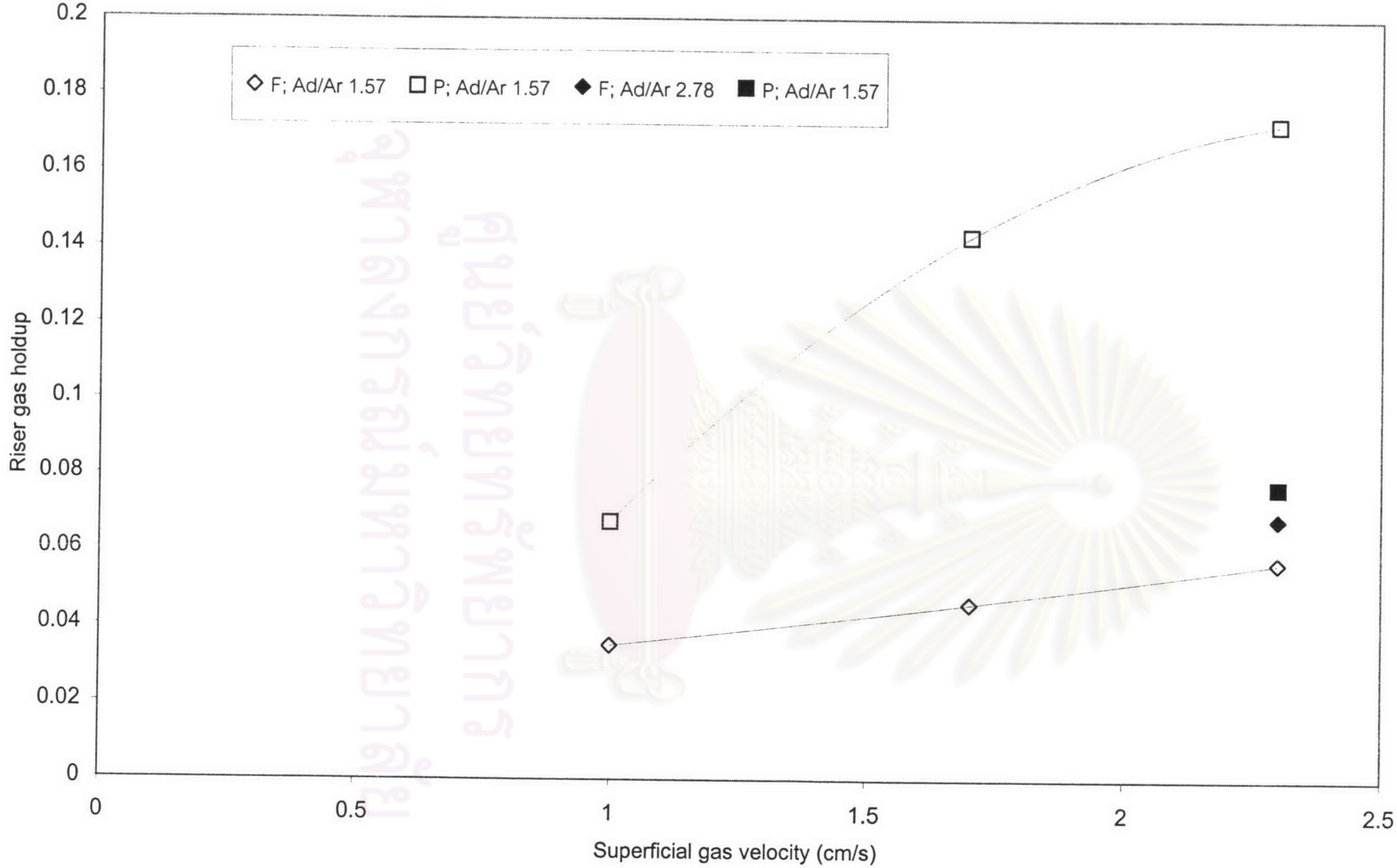

Figure 4.1 Relationship between riser gas holdup and superficial gas velocity for fluidized bed airlift filter and packed bed airlift filter

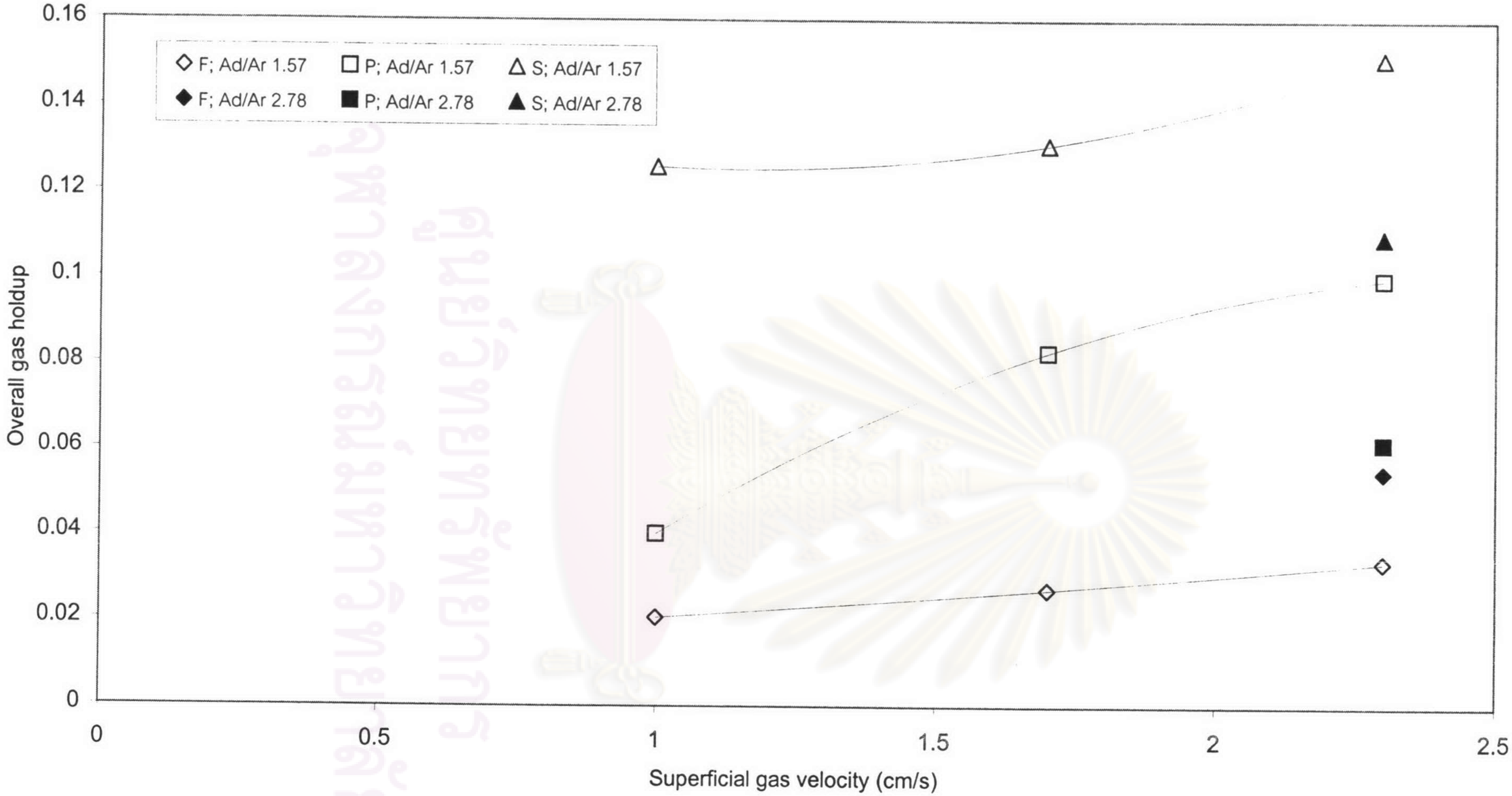

Figure 4.2 Relationship betwwwn overall gas holdup and superficial gas velocity for fluidized bed airlift filter, submerged filter and packed bed airlift filter

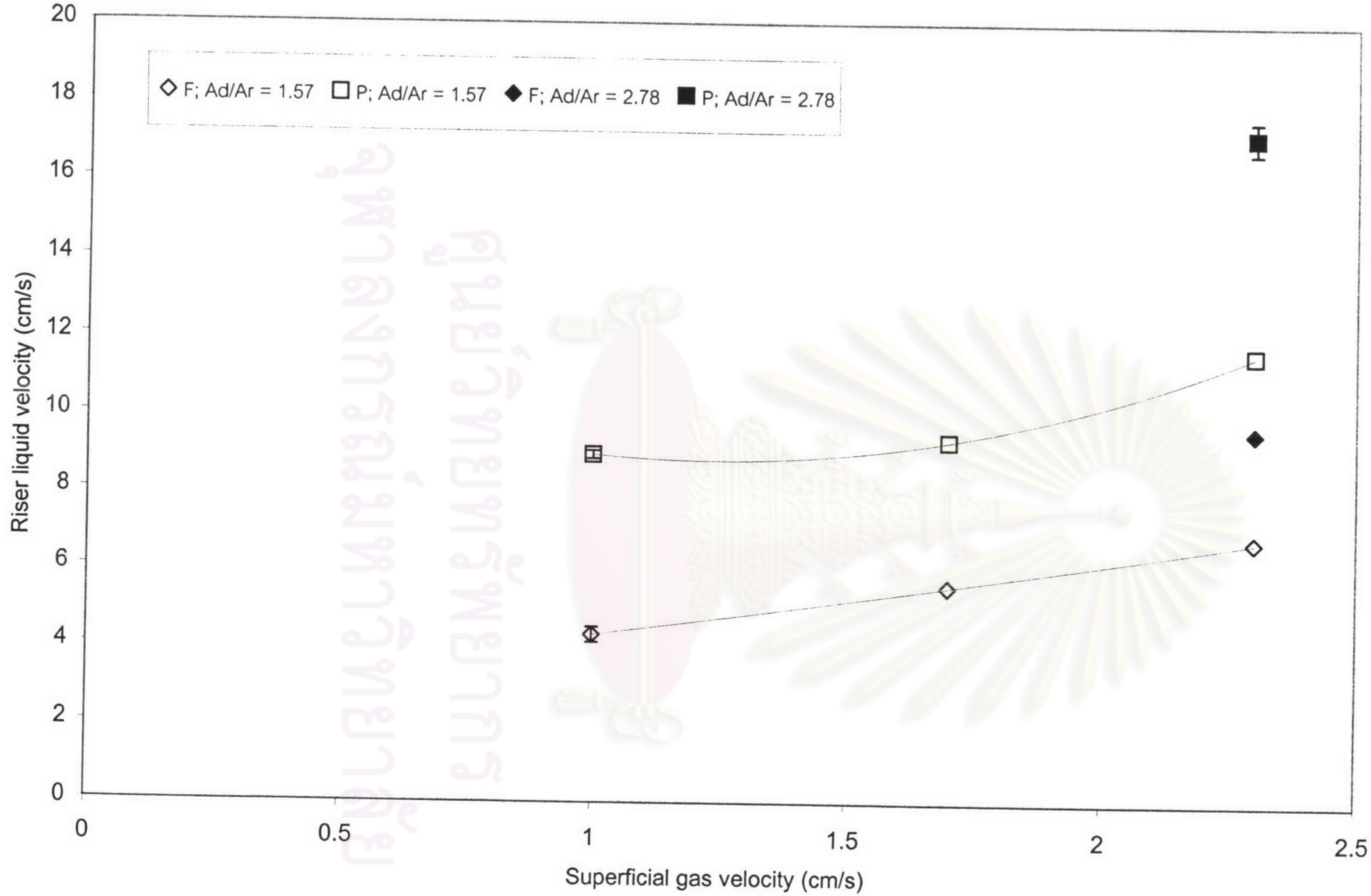

Figure 4.3 Relationship between riser liquid velocity and supficial gas velocity for fluidized bed airlift filter and packed bed airlift filter

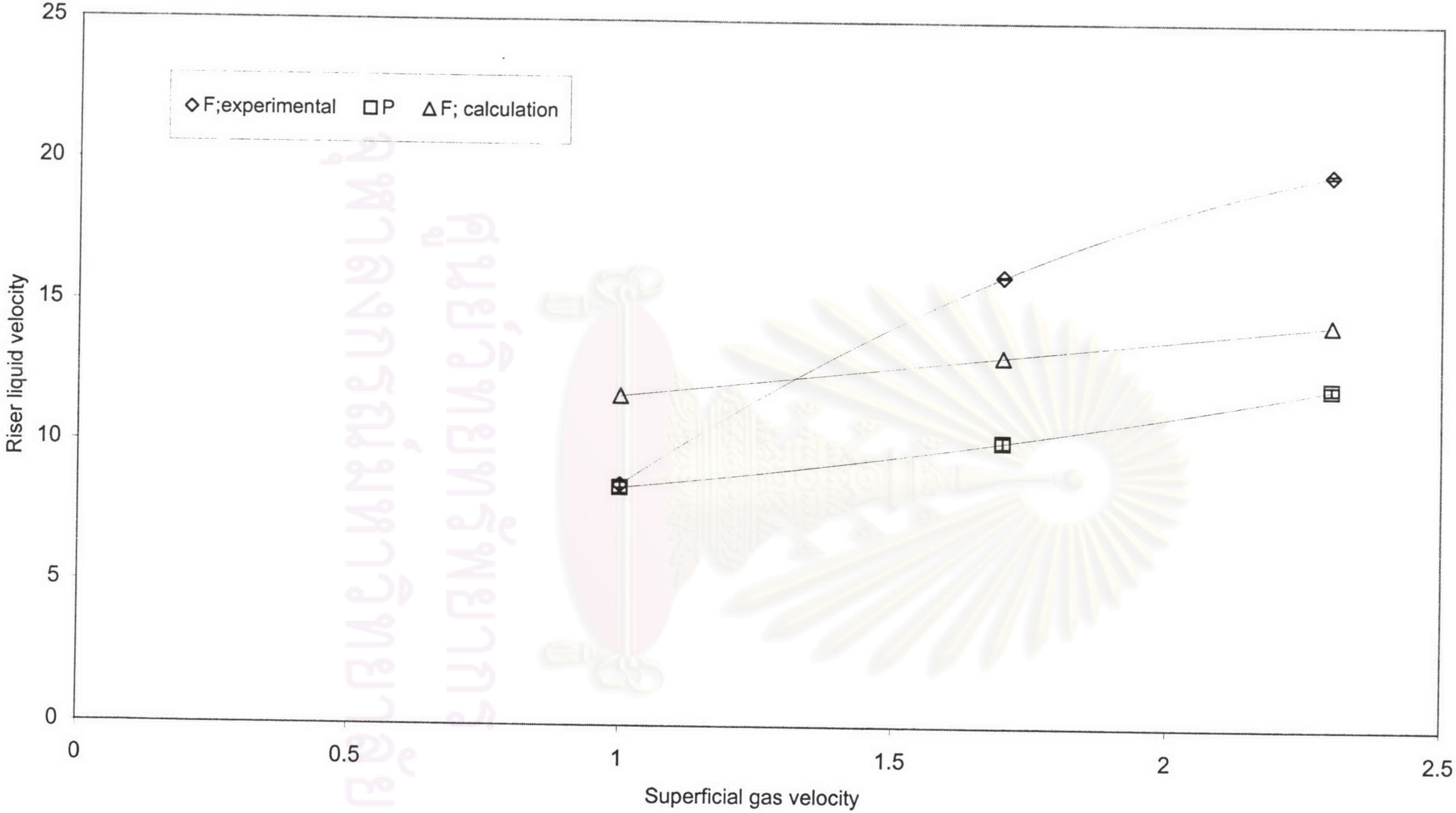

Figure 4.4 Relationship between riser liquid velocity and superficial gas velocity for fludized bed airlift filter and packed bed airlift filter (Ad/Ar=1.57)

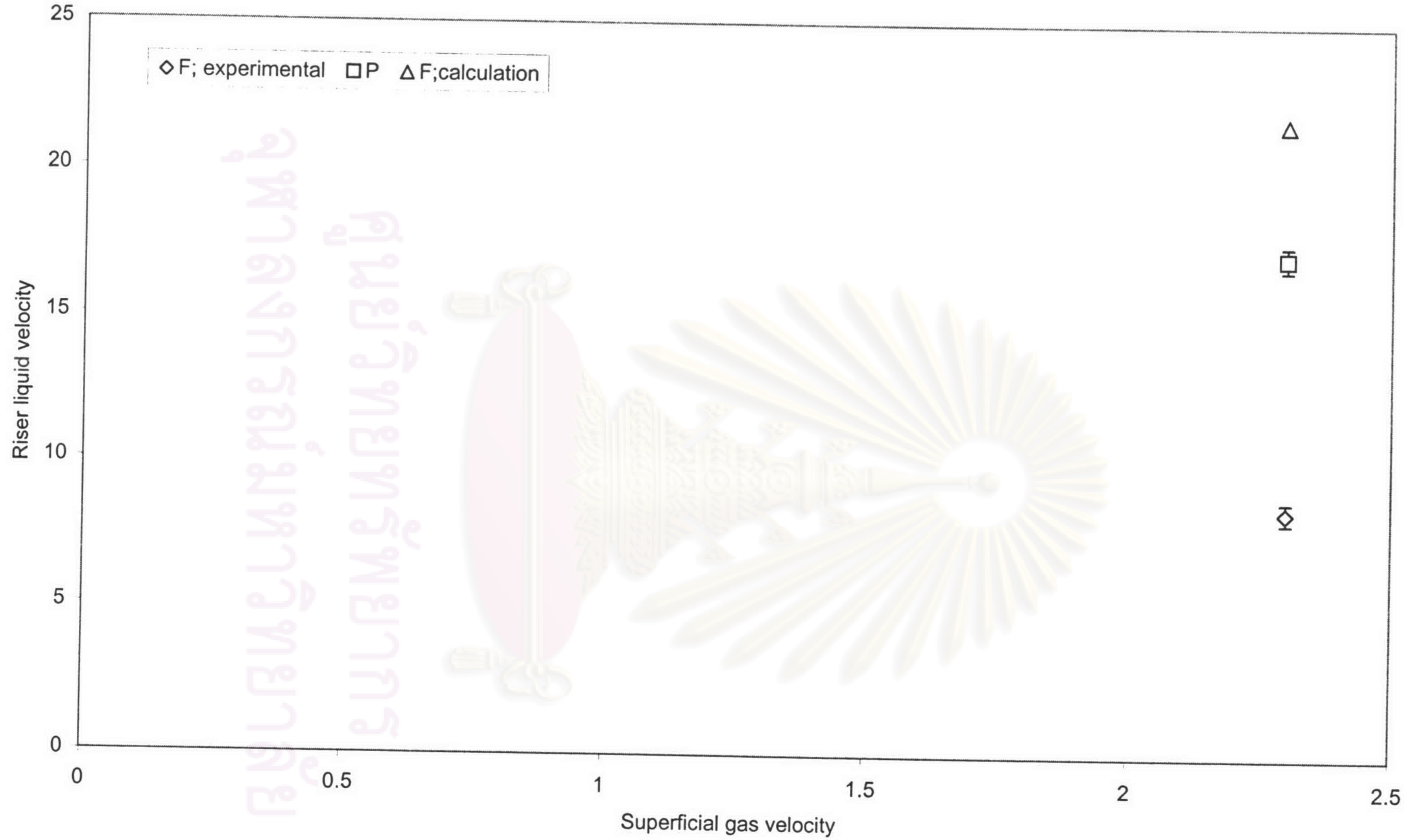

Figure 4.5 Relationship between riser liquid velocity and superficial gas velocity for fludized bed airlift filter and packed bed airlift filter (Ad/Ar=2.78)

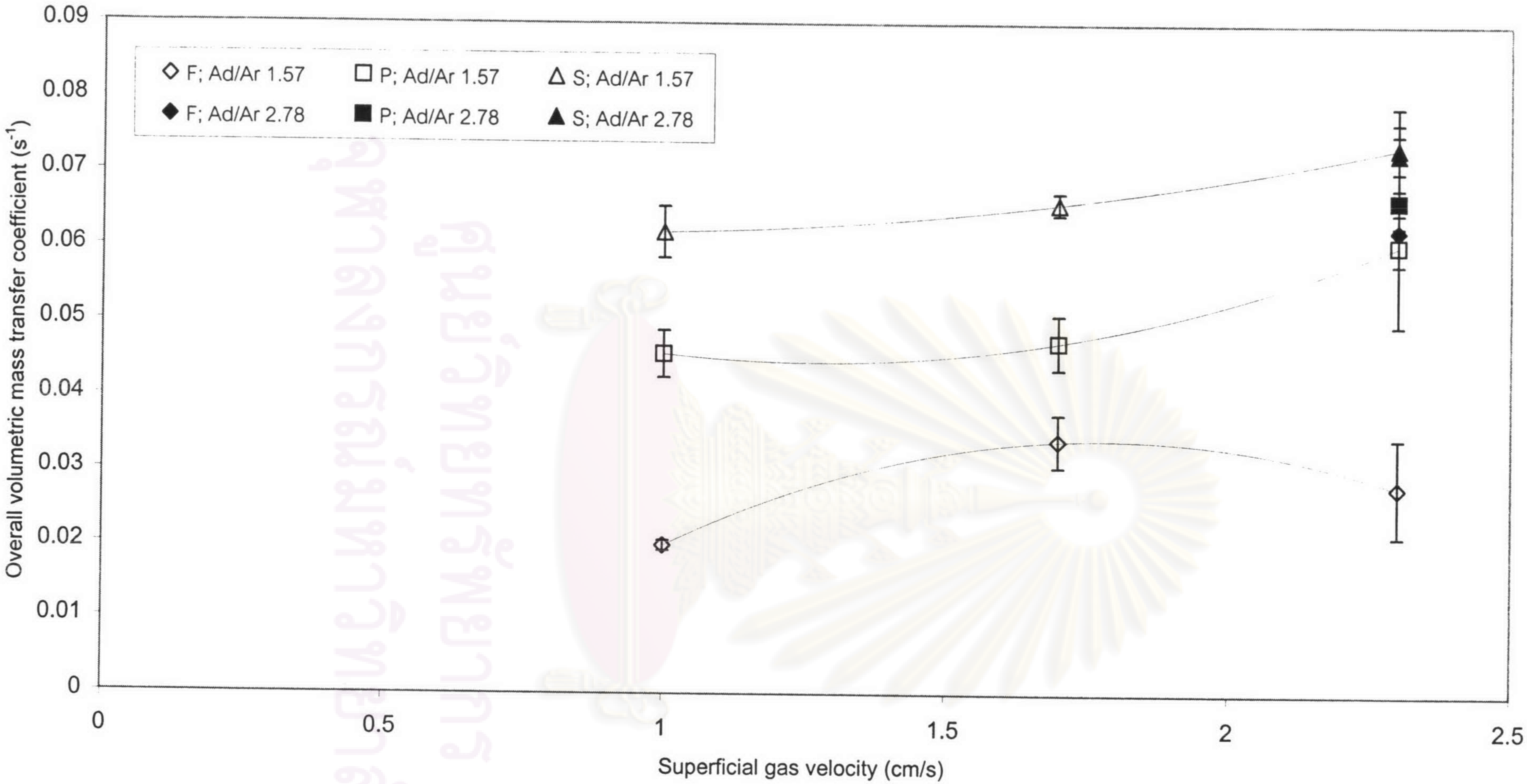

Figure 4.6 Relationship between overall volumetric mass tranfer coefficient for fluidized bed airlift filter, submerged filter and packed bed airlift filter

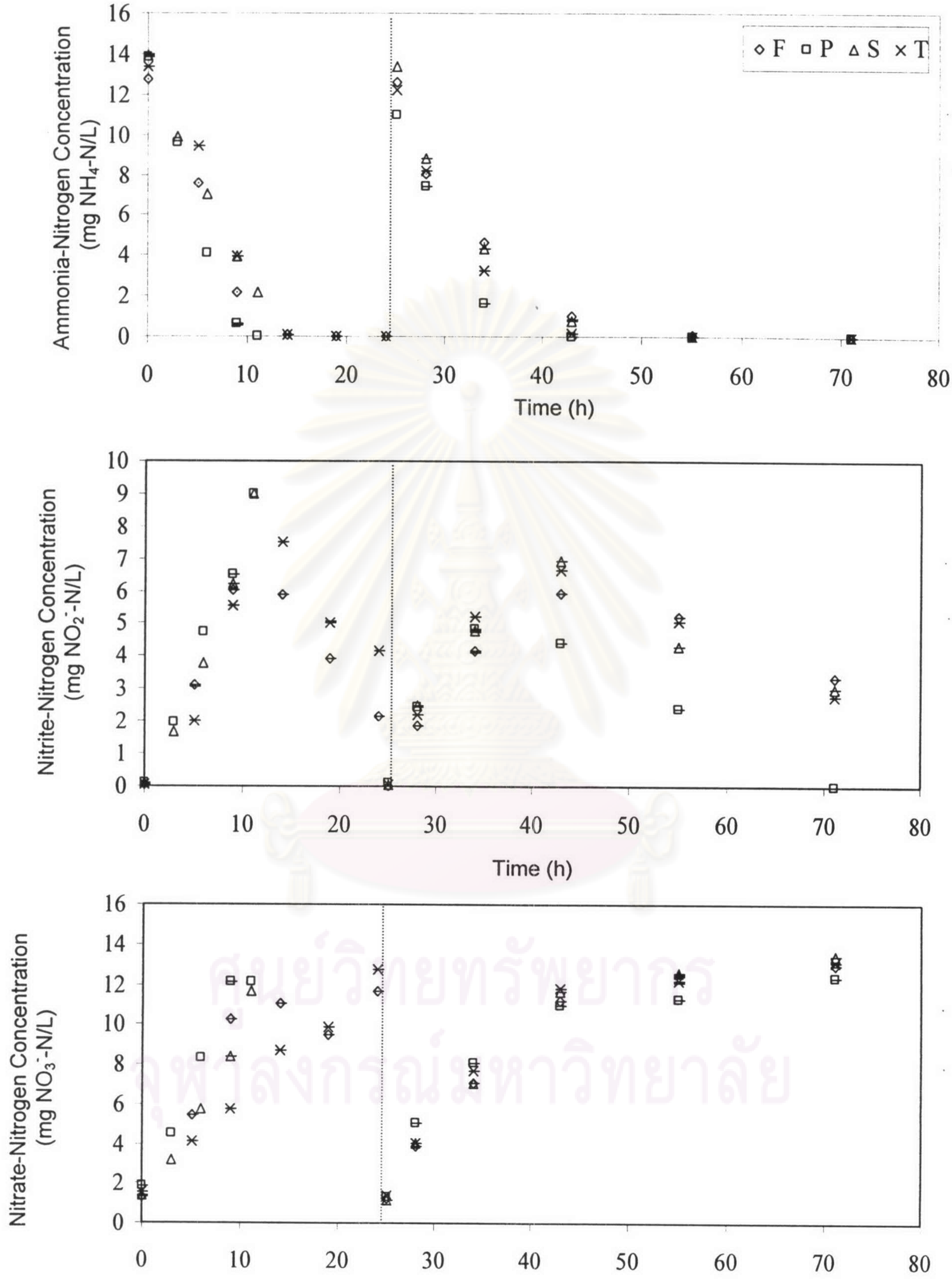

Figure 4.7 Nitrogen concentration profile in the fourth and fifth batch for fluidized bed airlift filter, submerged filter, packed bed airlift filter and trickling filter (A_d/A_r 1.57 , Usg 1.7 cm/s)

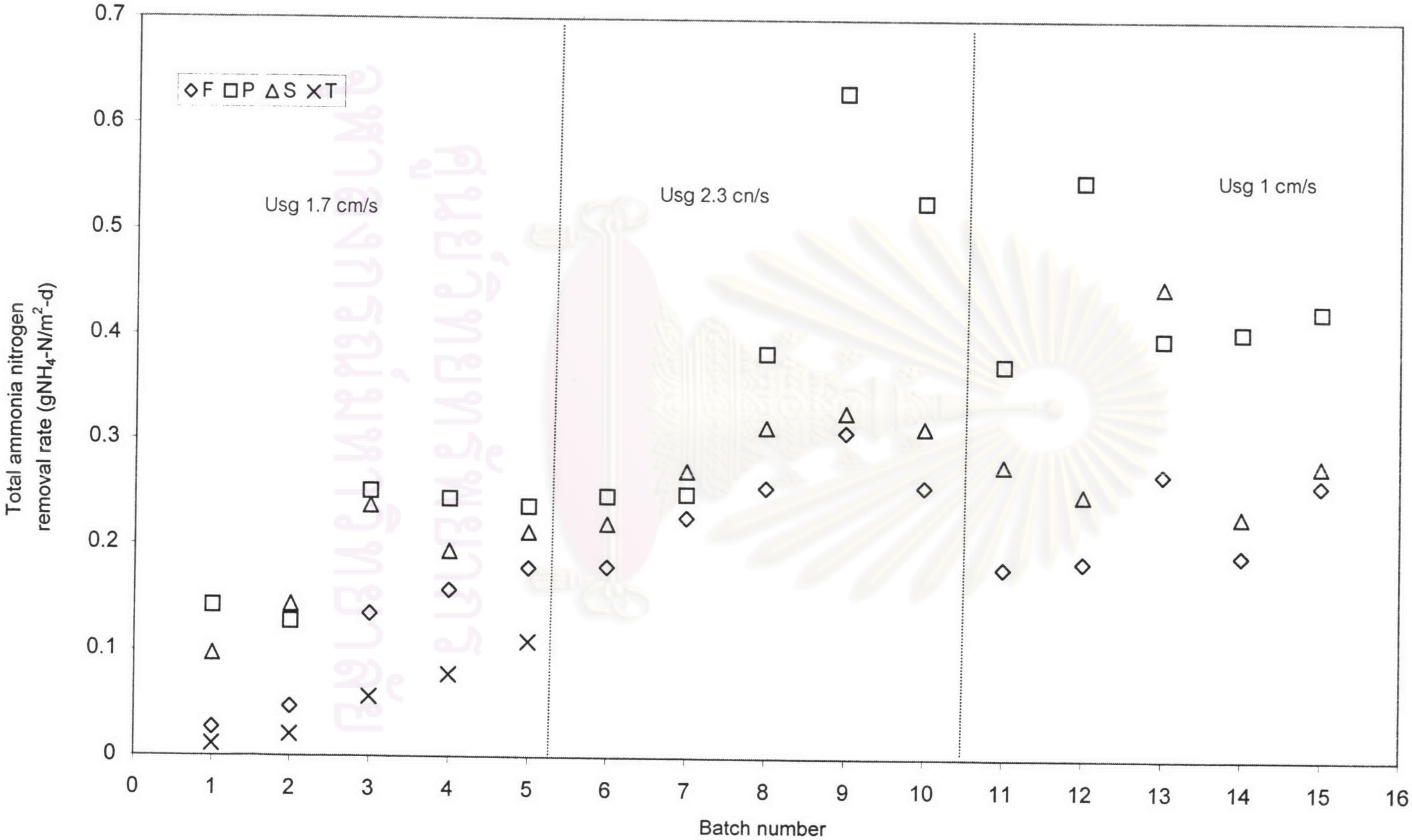

Figure 4.8 Total ammonia removal rate for fluidized bed airlift filter, packed bed airlift filter, submerged filter and trickling filter (A_d/A_r=1.57)

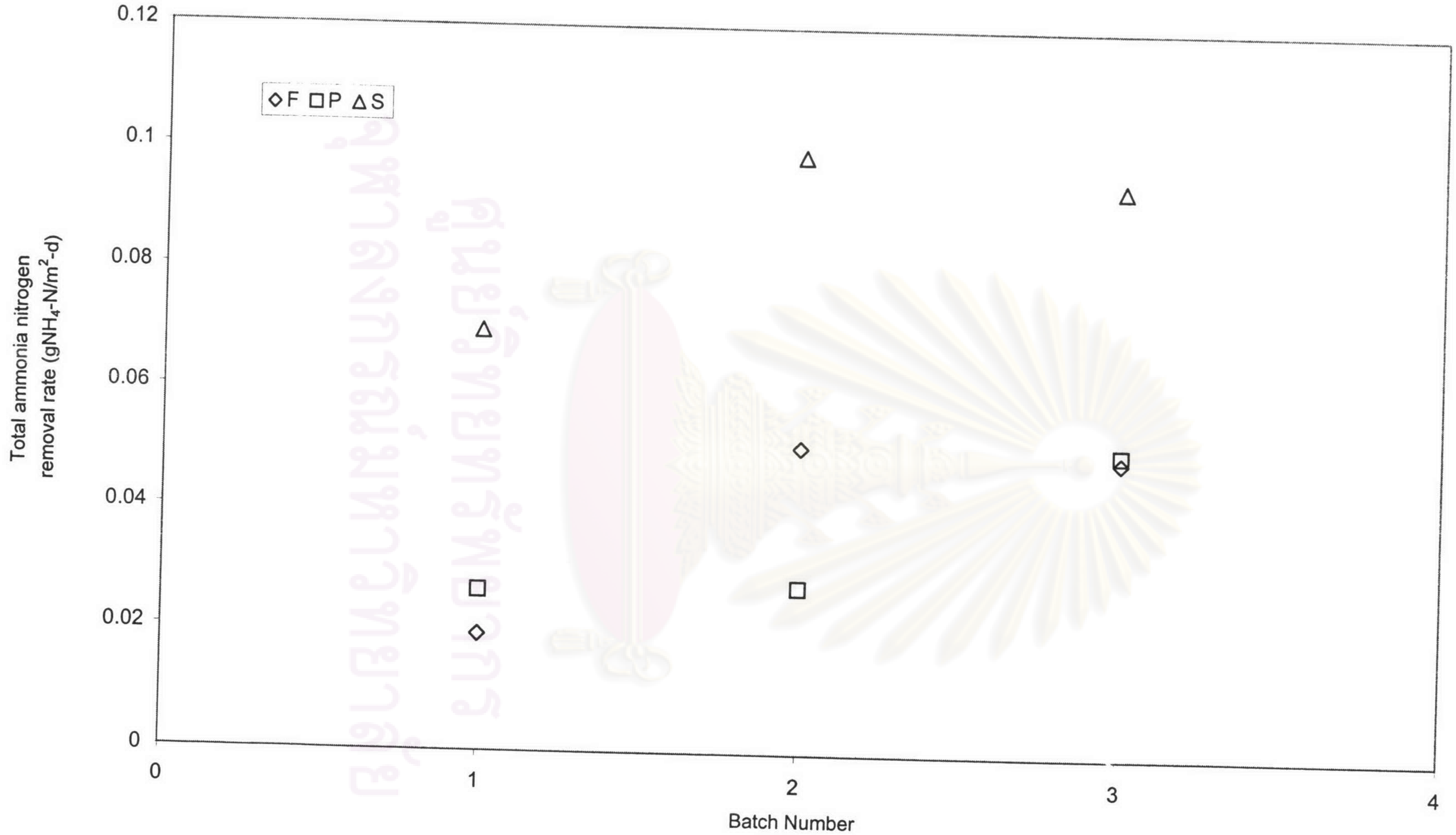

Figure 4.9 Total ammonia removal rate for fluidized bed airlift filter, packed bed airlift filter and submerged filter (A_d/A_r=2.78)

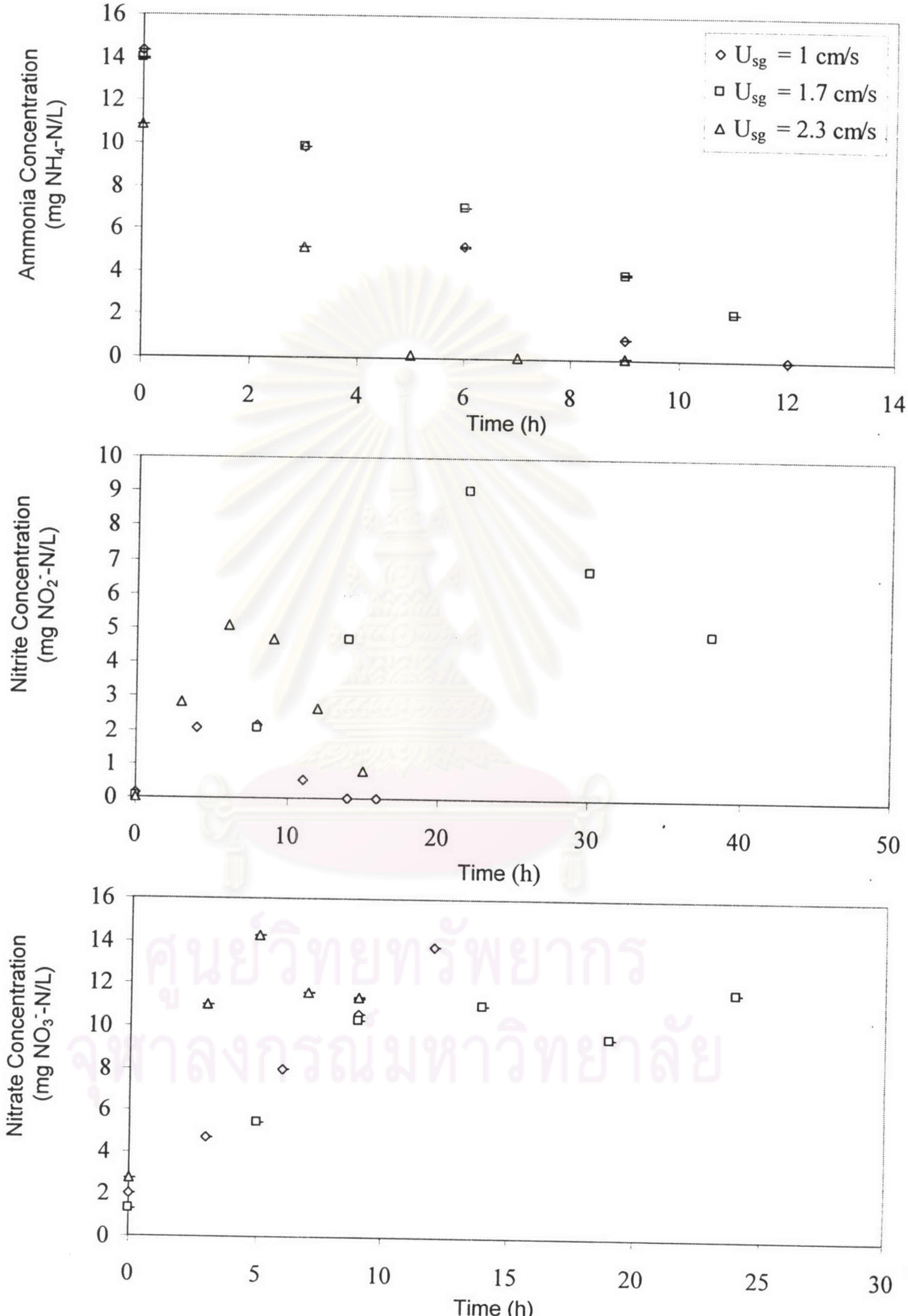

Figure 4.10 Nitrogen concentration as a result of various superficial gas velocity in fourth batch airlift fluidized bed reactor (F). (A_d/A_r=1.57)

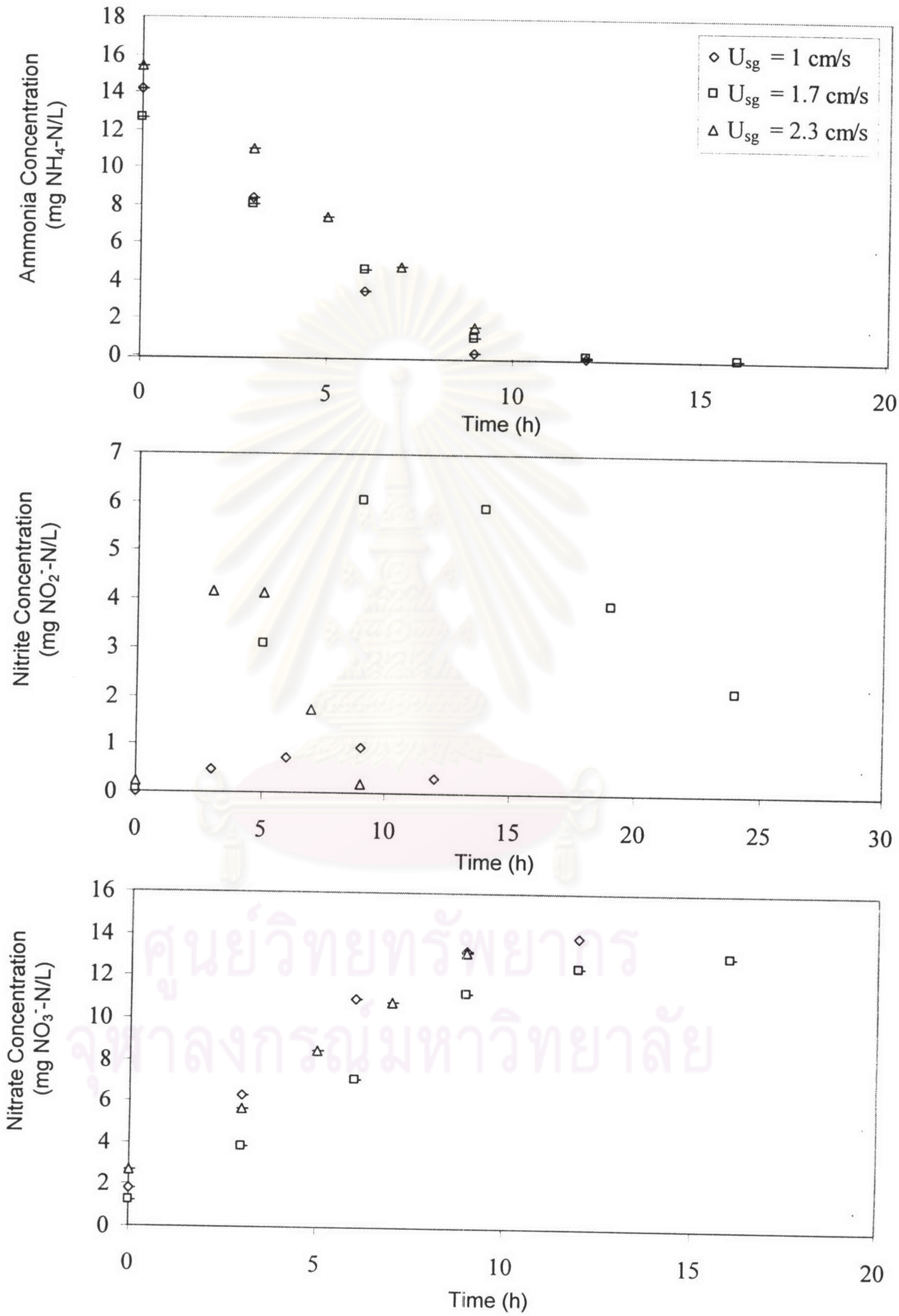

Figure 4.11 Nitrogen concentration as a result of various superficial gas velocity in fifth batch airlift fluidized bed reactor (F). (A_d/A_r=1.57)

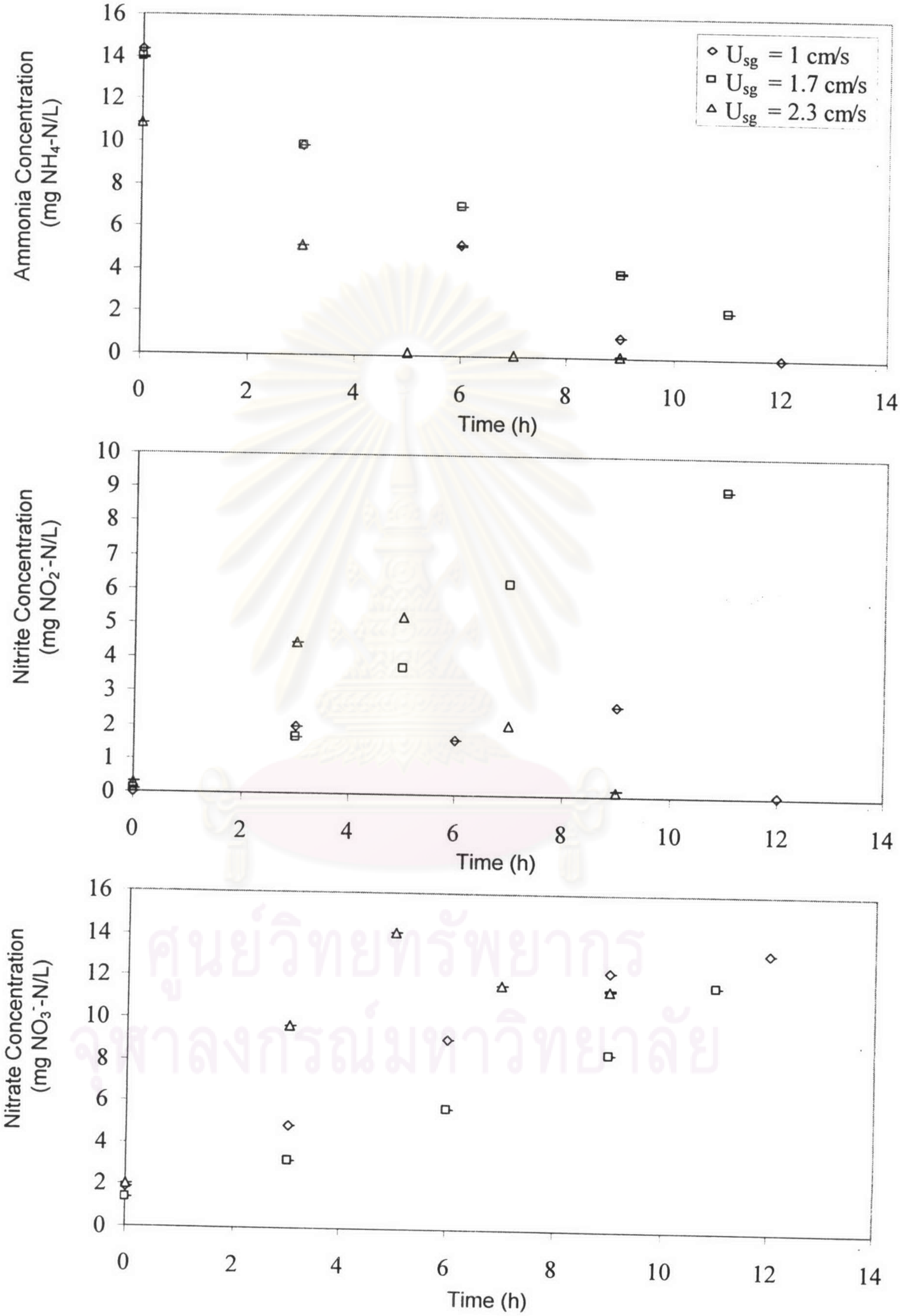

Figure 4.12 Nitrogen concentration as a result of various superficial gas velocity in fourth batch submerged filter (S). (200 bioball)

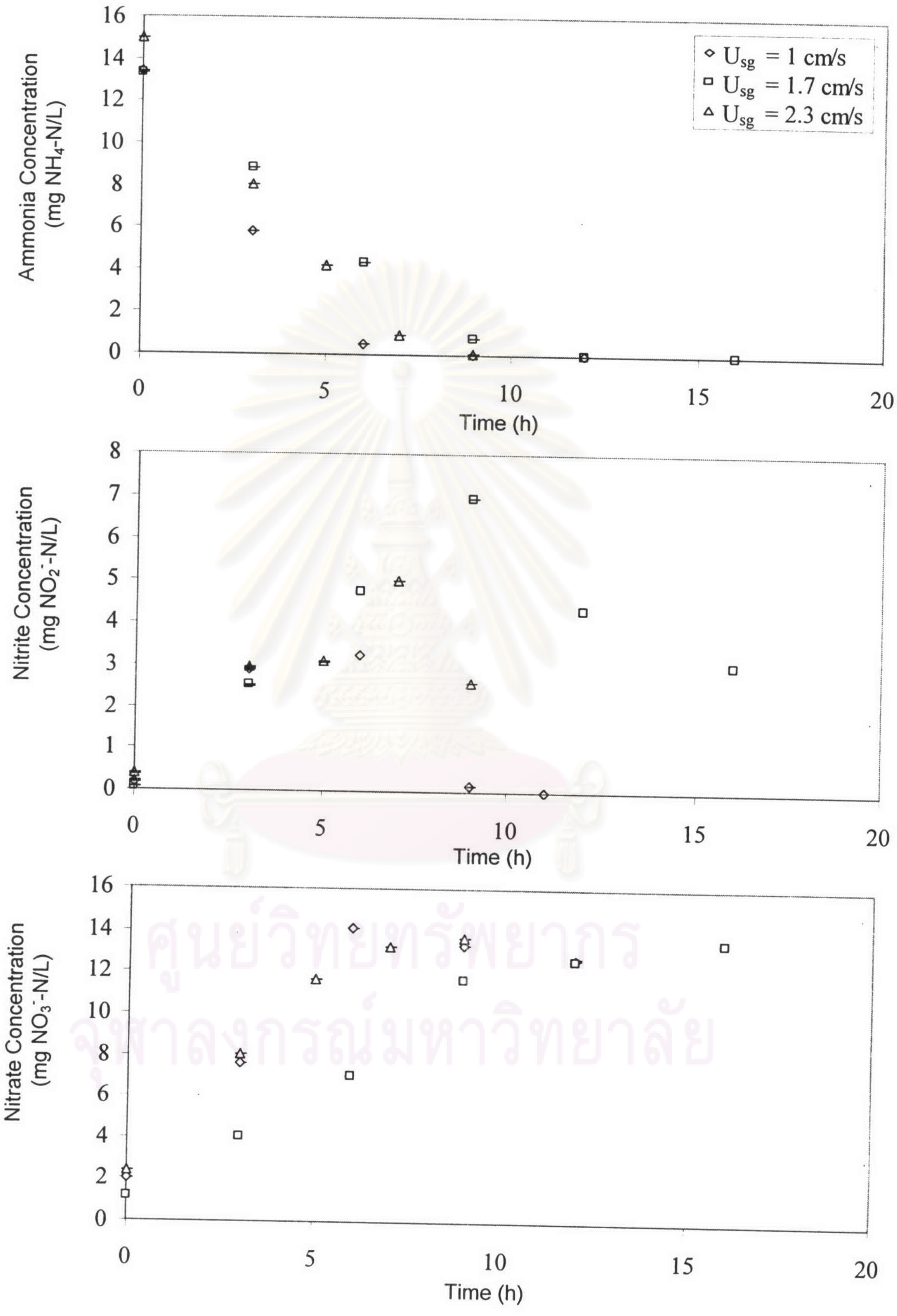

Figure 4.13 Nitrogen concentration as a result of various superficial gas velocity in fifth batch submerged filter (S). (200 bioball)

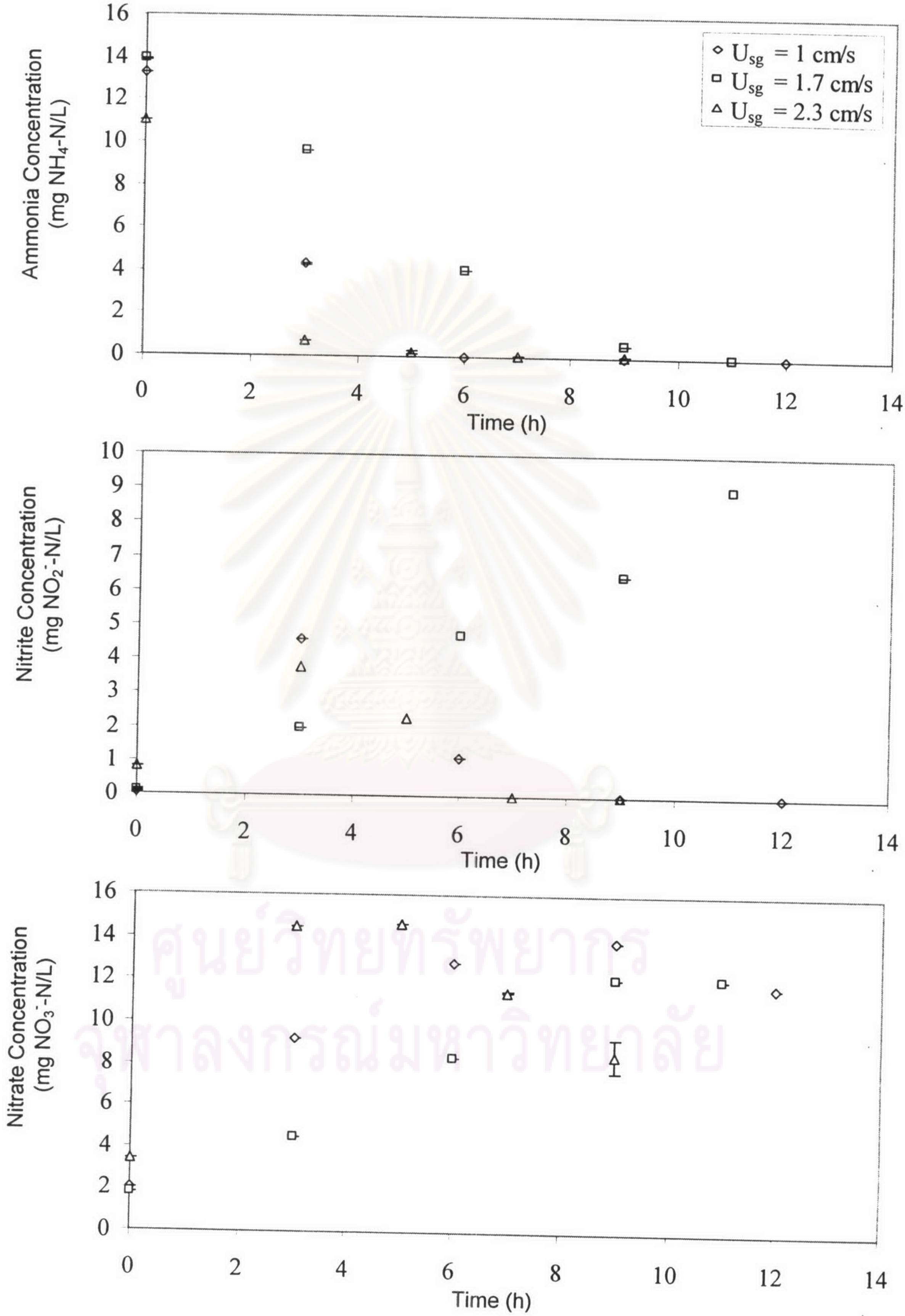

Figure 4.14 Nitrogen concentration as a result of various superficial gas velocity in fourth batch airlift packed bed reactor (P). (A_d/A_r =1.57)

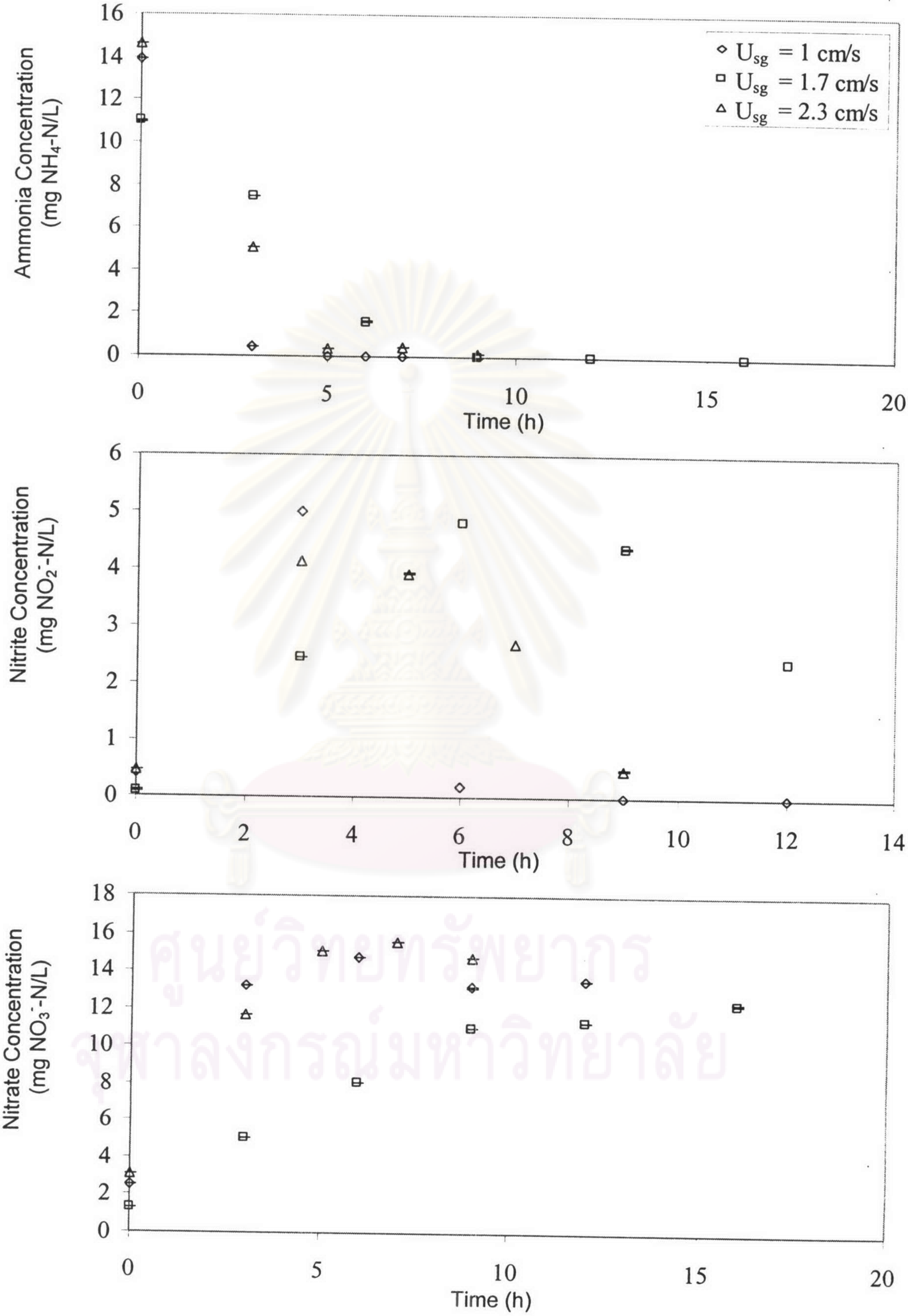

Figure 4.15 Nitrogen concentration as a result of various superficial gas velocity in fifth batch airlift packed bed reactor (P). (A_d/A_r =1.57)